Research in Astron. Astrophys. **2012** Vol. **12** No. **2**, 147–157
http://www.raa-journal.org *http://www.iop.org/journals/raa*

***R**esearch in*
***A**stronomy and*
***A**strophysics*

Radio observations of the first three-months of *Fermi* AGN at 4.8 GHz *

Xiang Liu[1], Hua-Gang Song[1,2], Jun Liu[1], Zhen Ding[1], Nicola Marchili[3], Thomas P. Krichbaum[3], Lars Fuhrmann[3], Anton Zensus[3] and Tao An[4]

[1] Xinjiang Astronomical Observatory, Chinese Academy of Sciences, Urumqi 830011, China; *liux@xao.ac.cn*
[2] Graduate University of Chinese Academy of Sciences, Beijing 100049, China
[3] Max-Plank-Institut für Radioastronomie, Auf dem Hügel 69, 53121 Bonn, Germany
[4] Shanghai Observatory, Chinese Academy of Sciences, Shanghai 200030, China

Received 2010 August 30; accepted 2011 October 7

Abstract Using the Urumqi 25 m radio telescope, sources from the first three months of the *Fermi*-large area telescope detected active galactic nuclei (AGN) catalog with a declination of $> 0^\circ$ were observed in 2009 at 4.8 GHz. The radio flux density appeared to correlate with the γ-ray intensity. Intra-day variability (IDV) observations were performed in March, April and May 2009 for 42 selected γ-ray bright blazars, and $\sim$60% of them showed evidence of flux variability at 4.8 GHz during the IDV observations. The IDV detection rate was higher than that in previous flat-spectrum AGN samples. IDV appeared more often in the very long baseline interferometry-core dominant blazars, and the non-IDV blazars showed relatively "steeper" spectral indices than the IDV blazars. Pronounced inter-month variability was also found in two BL Lac objects: J0112+2244 and J0238+1636.

Key words: galaxies: active — quasars: general — radio continuum: galaxies — gamma-rays: observations

1 INTRODUCTION

In the 1990s, the space γ-ray telescope EGRET (Energetic Gamma Ray Experiment Telescope) identified 66 blazars during its mission (Hartman et al. 1999). *Fermi* (the Fermi Gamma Ray Space Telescope), the successor of EGRET, launched in 2008, is now conducting an all-sky survey mission. *Fermi* has a much higher sensitivity and pointing accuracy than EGRET, and has already detected more active galactic nuclei (AGNs), see Abdo et al. (2010). The first three months of observations with the *Fermi*-LAT (the large area telescope on-board the Fermi spacecraft) detected 132 bright γ-ray sources, of which 104 were blazars (Abdo et al. 2009). Some of the *Fermi*-LAT detected AGNs exhibit γ-ray variability on a timescale of days.

Blazars are either flat-spectrum radio quasars or BL Lac objects, and they are extremely variable at all observable wavelengths on timescales ranging from less than an hour to many years, both in

* Supported by the National Natural Science Foundation of China.

total power and linear polarization. The apparent motions of VLBI (very long baseline interferometry) components along their jets are often highly superluminal with brightness temperatures being close to the inverse-Compton limit. Such violent blazar behavior is attributed to relativistic jets oriented close to the line of sight (Rees 1966; Urry & Padovani 1995). The relationship of variability at different wavelengths is a crucial test for theoretical models of these outbursts/flares in γ-ray AGNs.

Although it is generally accepted that the γ-rays detected from blazars are emitted from collimated jets of charged particles moving at relativistic speeds (Maraschi et al. 1992), some open questions remain. The mechanisms by which the particles are accelerated, the precise site of the γ-ray production, the origin of AGN variability and the γ-ray duty cycle of blazars are still not well understood.

Intra-day variability (IDV: rapid variability on timescales of a few hours to a few days) observation and radio monitoring can provide the variability characteristics of AGNs in radio, allowing us to search for correlations between radio and γ-ray luminosities and to study the connection between the emission mechanisms.

The IDV of radio flux density has been found in about 30% to 50% of flat-spectrum radio sources (Quirrenbach et al. 1992; Lovell et al. 2008). If interpreted as being source-intrinsic, the rapid variability would imply micro-arcsecond scale sizes of the emitting regions, which would result in excessively large apparent brightness temperatures far in excess of the inverse-Compton limit of $\sim 10^{12}$ K (Kellermann & Pauliny-Toth 1969; Readhead 1994). Thus, theories which explain IDV with variations intrinsic to the blazars require either excessively large Doppler boosting factors or special source geometries (such as non-spherical relativistic emission models, e.g. Qian et al. 1996) or coherent and collective plasma emission (Benford 1992; Lesch & Pohl 1992) to avoid the inverse-Compton catastrophe. Alternatively, IDV was explained by interstellar scintillation (ISS), especially for very rapid variables such as PKS 0405$-$385, J1819+384, PKS 1257$-$326 and J1128+592 (Kedziora-Chudczer et al. 1997; Dennett-Thorpe & de Bruyn 2000; Bignall et al. 2003; Gabányi et al. 2009, respectively).

Almost all the *Fermi*-LAT detected AGNs are blazars. There appears to be a significant correlation between the radio flux density at 15 GHz and the γ-ray flux density of the *Fermi*-LAT AGN (Ackermann et al. 2011). It is expected that the *Fermi* AGNs are more IDV-active than non γ-ray AGNs. Dedicated IDV and flux density monitoring observations are needed to study the variability on different timescales and to correlate the occurrence of IDV with the γ-ray activity of the *Fermi* AGNs. In March 2009 we launched a program with the 25-m Urumqi radio telescope at 4.8 GHz to investigate the intra-day to inter-month variability of the first three months of *Fermi* detected AGNs. The aim was to search for new IDV sources and for a statistical comparison of the radio and γ-ray emission of *Fermi* detected AGNs.

In this paper, we present the results from our single-dish radio observations of the *Fermi*-LAT detected AGNs with a declination of $> 0^\circ$. We adopt $S \propto \nu^\alpha$ to define a spectral index throughout the paper.

2 SAMPLE AND OBSERVATIONS

Our sample is selected from the catalog of the first three months of *Fermi*-LAT-detected AGNs (Abdo et al. 2009). We originally observed 63 sources with a declination of $> 0^\circ$ from the catalog as our pilot "cross-scan" observation in March 2009. Thirteen sources were rejected due to poor data quality in the pilot run. The flux densities of 50 sources were obtained in the pilot observation at 4.8 GHz, including galaxy NGC 1275 (3C 84). We selected the sources for IDV observation from the 50 sources by the following criteria:

(1) Blazars with source brightness: $S_{4.8\mathrm{GHz}} >$0.3 Jy.
(2) Source compactness: measured full-width-half-maximum of source brightness profile $<700''$, which is $\sim$1.2 times the antenna beam size at 4.8 GHz. The extended source brightness profile

may indicate a confusion between the target and its nearby sources which cannot be resolved by the 25-m radio telescope at 4.8 GHz.

The criteria restricted the number of sources for IDV observation to be 45. Unfortunately, three of them, namely J0920+4441, J1229+0203 (3C 273) and J1253+5301, were not involved in the subsequent IDV campaign by mistake. Therefore, there were 42 sources on which IDV observations were made, which consisted of 24 flat-spectrum radio quasars and 18 BL Lac objects.

IDV observations were carried out in order to study the short time-scale variability of the γ-ray bright blazars. These sources were also planned to be monitored monthly from March to December in 2009 at 4.8 GHz. Since all of the selected sources are strong and compact, both IDV observations and flux monitoring were performed in "cross-scan" mode.

2.1 IDV Observations

The three IDV observing sessions performed with the Urumqi telescope are summarized in Table 1: Col. 1 shows the symbols for the different epochs; Col. 2 the starting and ending dates of the experiments; Col. 3 the duration; Col. 4 the mean number of flux density measurements per hour; Col. 5 the number of observed sources (including the calibrators, we usually used 3C 286, 3C 48 and NGC 7027 as the primary calibrators, and B0836+710 and B0951+699, etc, as the secondary calibrators); Col. 6 the average number of measurements per hour for each *Fermi* blazar (duty cycle, which represents the shortest time scale on which we can search for variability); and Col. 7 the average modulation index of the calibrators, m_0, which is probably the most important since it reflects the conditions of the observation (the lower the m_0 the better the weather, and/or the more stable the receiver) and will be described in the following sections.

Table 1 Summary of the IDV Observations for the 42 Selected *Fermi* Blazars

Epoch	Date	Duration [d]	Average sampling [h^{-1}]	Number of observed sources	Duty cycle for *Fermi* blazars [h^{-1}]	m_0 [%]
(1)	(2)	(3)	(4)	(5)	(6)	(7)
A	21/03/09 – 25/03/09	4.8	11.2	49	0.3	0.6
B	19/04/09 – 24/04/09	5.3	10.8	37	0.4	0.7
C	06/05/09 – 09/05/09	3.8	10.1	17	0.8	0.6

2.2 Inter-month Observations

The 42-blazar sample was also planned to be monitored monthly from March to December in 2009 at 4.8 GHz. Each source was measured at least once in an individual observation. Sometimes the flux density measurements were repeated for sources whose observations were affected by adverse conditions such as bad weather and low elevation. Not all sources were actually observed every month due to time limitations, so some sources have no data in some months (in fact there are no data in June 2009 for all the sources).

3 DATA CALIBRATION

All observations were performed in the "cross-scan" mode with a central frequency of 4800 MHz and a bandwidth of 600 MHz; see Sun et al. (2007) for a description of the observing system. Each scan consists of eight sub-scans in azimuth and elevation over the source position, fourfold in each coordinate. This enables us to check the pointing offsets in both coordinates. After applying a correction for small pointing offsets, the amplitudes of both azimuth and elevation are averaged. Then, we correct the measurements for the elevation-dependent antenna gain and the remaining

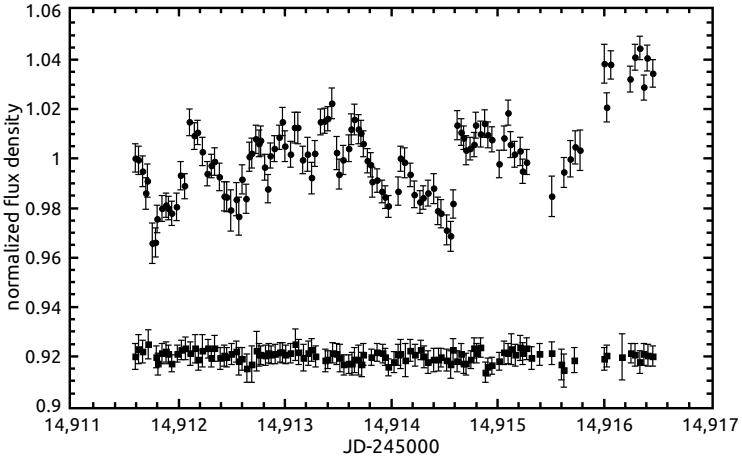

Fig. 1 Variability curve (normalized flux density $S/\langle S \rangle$ versus time) of J0721+7120 (B0716+714, *upper*), together with a nearby secondary calibrator B0951+699 (*lower*) in epoch A. The offset of the two curves is arbitrary, for better visualization.

Table 2 Flux Densities Measured for 10 Blazars but They Were not Involved in IDV Observations

Name/type	J0144+2705/BL	J0654+4514/Q	J0920+4441/Q	J0948+0022/Q	J1058+5628/BL
Alias	TXS 0141+268	B3 0650+453	RGB J0920+446	PMN J0948+0022	RXS J10586+5628
S (Jy)	0.240±0.003	0.449±0.003	1.058±0.006	0.191±0.006	0.189±0.007
Epoch	20090309	20090723	20090311	20090311	20090311
Name/type	J1229+0203/Q	J1253+5301/BL	J1542+6129/BL	J1959+6508/BL	J2325+3957/BL
Alias	3C 273	S4 1250+53	RXS J15429+6129	1ES 1959+650	B3 2322+396
S (Jy)	40.174±0.165	0.345±0.009	0.142±0.005	0.228±0.004	0.200±0.005
Epoch	20090311	20090311	20090919	20090309	20090819

systematic time-dependent effects by using a number of steep spectral and non-variable secondary calibrators. Finally, we convert our measurements to absolute flux density. The conversion factor is determined as the average scale of the frequently observed primary calibrator's assumed flux densities (Baars et al. 1977; Ott et al. 1994) by the measured temperatures, where we use the assumed flux densities of 7.53, 5.53 and 5.47 Jy at 4.8 GHz for the primary calibrators 3C 286, 3C 48 and NGC 7027, respectively in our data reduction.

The overall typical error of a single measurement is around 0.3%–1.5% of the source flux density, depending on, for example, weather conditions and source intensity; usually weaker sources have larger errors in individual measurements. Our data reduction of the radio flux density has essentially a similar procedure as the Effelsberg data reduction (e.g. Kraus et al. 2003). Actually, we have made simultaneous IDV observations with the Urumqi and Effelsberg telescopes as early as April 2006, and obtained consistent results between the two telescopes.

After the data reduction described above, the light curves of the sources were obtained. In Figure 1 we give an example of the variability curve after data calibration. We can see that the scatter of the calibrator is very small.

In addition, 11 sources have been measured for flux densities, but they were not involved in the IDV observations. The flux densities are useful in the correlation analysis between radio flux density and *Fermi* γ-ray intensity. So we list the source name/type (Q-quasar, BL-BL Lac object), flux density and observing epoch in Table 2, although three sources were measured for flux densities

in July, August and September 2009. The radio galaxy 3C 84 has a flux density of 16.174±0.065 Jy, measured on 2009 March 9, which is not listed in Table 2.

4 STATISTICAL ANALYSIS AND RESULTS

For the data analysis, we use several quantities such as the modulation index, the variability amplitude and so on. Here we just give a brief summary; a detailed description of these parameters can be found in Kraus et al. (2003).

(1) The modulation index m.
m is defined as the standard deviation of the flux density divided by the mean flux density of the source.

$$m[\%] = 100 \cdot \frac{\sigma_S}{\langle S \rangle},$$

where m provides a measure of the strength of the variations observed. One should notice that it does not account for the intrinsic noise in the data.

(2) The variability amplitude Y.
The noise-bias corrected variability amplitude Y is defined as

$$Y[\%] = 3\sqrt{m^2 - m_0^2},$$

where m_0 is the mean modulation index of all non-variable sources (see Heeschen et al. 1987), so it corresponds to the average residual noise and possibly even systematic scatter in the calibrators. Thus, compared to m_0, Y works as a more uniform estimator of the variability strength, and is useful for comparing data from different epochs.

(3) χ^2 and reduced χ^2.
As a criterion for the source variability, the hypothesis of a constant function is examined and the calibrated data are fitted by a χ^2 test of the kind

$$\chi^2 = \sum \left(\frac{S_i - \langle S \rangle}{\Delta S_i} \right)^2,$$

with the reduced χ^2

$$\chi_r^2 = \frac{1}{N-1} \cdot \sum \left(\frac{S_i - \langle S \rangle}{\Delta S_i} \right)^2,$$

where S_i denotes the individual flux densities, $\langle S \rangle$ their average in time, ΔS_i their errors and N the number of measurements (e.g. Bevington & Robinson 1992). Only those sources for which the probability that they can be fitted by a constant function is $\leq 0.1\%$ are considered to be variable.

We define the modulation index M for the inter-month flux density variations similar to m for the IDV. For the calibrators we obtain $M_0 \sim 2$ [%]. Because the inter-month data are sparse and unevenly sampled, we treat the M_0 as the error of M, and do not define a noise-bias corrected Y for the inter-month data.

Here, we present the basic information of the sources, and the statistical results of the IDV and inter-month observations at 4.8 GHz in Table 3. The different columns are assigned as follows: column (1) source J2000 name; (2) alias; (3) optical identification (Q: quasar, BL: BL Lac object) and VLBI structure (c: extremely core dominated, cj: core with a mild jet); (4) spectral index from the SPECFIND V2.0 catalog of broad-band radio spectra (Vollmer et al. 2010), using a least squares

Table 3 Results of IDV and Inter-month Radio Observations

Source (1)	alias (2)	Id/vlbi (3)	$\alpha1/\alpha2$ (4)	Ep (5)	N (6)	$\overline{S}$ [Jy] (7)	m [%] (8)	χ^2_r (9)	Y [%] (10)	IDV (11)	$\overline{S_M}$ [Jy]/M[%] (12)	No. (13)
J0112+2244	S2 0109+22	BL/c	0.18[a]/0.12	A	10	0.756	3.02	16.42	8.89	+	0.508/37.1	7
				B	10	0.674	6.21	30.56	18.51	+		
J0136+4751	DA 55	Q/c	0.10/0.19	A	13	4.320	1.18	9.93	3.04	+	4.044/6.6	8
J0217+0144	PKS 0215+015	Q/c	0.16/0.24	A	7	1.298	2.17	12.74	6.24	+	1.284/7.0	7
				B	14	1.288	3.75	23.88	11.06	+		
J0238+1636	AO 0235+164	BL/c	0.26/0.56	A	10	3.331	1.00	7.03	2.40	+	2.225/42.7	7
J0530+1331	PKS 0528+134	Q/cj	0.44[a]/0.24	A	9	3.490	0.34	0.75	0.00		3.121/9.9	8
				B	15	3.587	2.95	34.38	8.61	+		
J0654+5042		Q/cj	0.30[a]/0.23	A	9	0.315	1.57	1.23	4.37		0.313/10.2	7
				B	20	0.303	2.76	2.98	8.01	+		
J0712+5033		BL/c	0.37[a]/0.40	A	12	0.313	2.79	4.13	8.17	+	0.315/9.4	2
				B	25	0.349	3.39	5.01	9.94	+		
J0713+1935		Q/c	0.16[b]/0.35	A	9	0.276	6.81	17.04	20.34	+	0.254/19.1	2
				B	15	0.451	6.99	34.75	20.87	+		
J0719+3307	TXS 0716+332	Q/c	–0.20/–0.15	A	10	0.509	2.17	4.98	6.26	+	0.546/6.9	2
				B	24	0.595	3.83	13.53	11.30	+		
J0721+7120	S5 0716+71	BL/c	–0.43[c]/–0.13	A	117	1.241	1.61	8.34	4.48	+	1.305/18.4	9
				B	92	1.361	3.66	37.68	10.77	+		
				C	85	1.134	3.35	25.11	9.90	+		
J0738+1742	PKS 0735+178	BL/cj	–0.01/0.27	A	8	0.902	0.54	0.68	0.00		0.915/2.0	2
				B	16	0.935	2.75	14.26	7.97	+		
J0818+4222	OJ 425	BL/cj	–0.10/–0.04	A	10	1.503	1.90	15.73	5.40	+	1.660/11.9	8
				B	24	1.522	2.03	8.07	5.71	+		
J0824+5552	TXS 0820+560	Q/cj	–0.08/0.10	A	13	1.049	0.59	0.92	0.00		1.083/6.7	7
				B	28	1.048	0.66	0.66	0.00			
J0854+2006	OJ 287	BL/cj	0.35/0.44	A	8	1.952	1.56	12.16	4.31	+	1.911/5.1	2
J0957+5522	4C +55.17	Q/cj	–0.34[c]/–0.41	A	13	1.939	0.15	0.08	0.00		1.980/4.6	8
				B	26	1.937	0.30	0.28	0.00			
J1015+4926	1ES 1011+496	BL/cj	–0.21/–0.24	A	10	0.358	1.48	1.15	4.04		0.352/4.0	4
				B	19	0.356	1.50	1.06	3.99			
J1016+0513	PMN J1016+0512	Q/cj	–0.07[a]/–0.18	A	4	0.533	1.43	2.56	3.90		0.593/5.9	3
J1033+6051	S4 1030+61	Q/cj	–0.21[c]/–0.05	A	17	0.427	2.99	5.22	8.77	+	0.382/16.7	7
				B	34	0.412	2.89	4.61	8.41	+		
J1104+3812	Mrk 421	BL/cj	–0.25/–0.11	A	8	0.590	1.03	1.36	2.51		0.596/3.0	5
J1159+2914	4C +29.45	Q/c	–0.29/–0.29	A	62	2.733	1.86	14.31	5.29	+	2.702/2.6	2
				B	55	2.627	1.30	4.69	3.29	+		
J1217+3007	B2 1215+30	BL/cj	–0.33/–0.30	A	10	0.443	1.41	1.39	3.82		0.452/7.8	5
				B	19	0.441	1.55	1.54	4.13			
J1221+2813	W Com	BL/cj	0.07/0.19	A	11	0.481	1.82	2.58	5.17		0.491/2.0	2
J1310+3220	B2 1308+32	Q/cj	0.09/0.30	A	9	1.054	2.00	7.06	5.73	+	1.222/8.7	6
				B	18	1.092	1.24	2.73	3.06	+		
J1427+2348	PKS 1424+240	BL/cj	–0.33/–0.34	A	10	0.362	2.20	2.38	6.36		0.340/1.5	3
				B	19	0.355	1.83	1.47	5.07			
				C	2	0.359	1.16	0.27	2.96			
J1504+1029	PKS 1502+106	Q/cj	0.06/–0.03	A	8	1.524	0.63	0.77	0.54		1.601/8.2	9
				B	14	1.611	0.86	1.58	1.50			
				C	31	1.725	0.94	1.98	2.17			
J1522+3144	TXS 1520+319	Q/c	–0.14/0.18	A	9	0.536	0.55	0.39	0.00		0.528/7.9	8
				C	33	0.512	2.60	4.61	7.60	+		
J1553+1256	PKS 1551+130	Q/cj	–0.26/–0.47	A	8	0.703	0.48	0.10	0.00		0.723/9.3	8
				C	29	0.721	1.37	2.40	3.71	+		
J1555+1111	PG 1553+11	BL/c	0.04/0.26	C	13	0.315	2.79	1.46	8.18		0.298/4.8	4
J1635+3808	4C +38.41	Q/cj	–0.01/–0.09	A	11	2.894	0.33	0.53	0.00		3.165/10.6	8
				B	21	2.931	0.38	0.55	0.00			
				C	33	3.013	0.45	0.76	0.00			

Table 3 – *Continued.*

Source (1)	alias (2)	Id/vlbi (3)	$\alpha 1/\alpha 2$ (4)	Ep (5)	N (6)	$\overline{S}$ [Jy] (7)	m [%] (8)	χ^2_r (9)	Y [%] (10)	IDV (11)	$\overline{S_M}$ [Jy]/M[%] (12)	No. (13)
J1653+3945	Mrk 501	BL/cj	–0.12/–0.19	A	10	1.535	0.58	0.95	0.00		1.573/7.7	8
				C	32	1.539	0.60	0.73	0.00			
J1719+1745	PKS 1717+177	BL/cj	0.21[a]/0.03	A	10	0.592	2.64	5.12	7.72	+	0.621/8.5	7
				B	19	0.590	1.77	3.16	4.87	+		
				C	27	0.603	1.48	2.11	4.06	+		
J1751+0939	OT 081	BL/c	0.41[a]/0.64	A	10	2.872	1.37	9.51	3.69	+	3.204/16.8	3
				C	27	2.572	1.36	7.32	3.67	+		
J1800+7828	S5 1803+78	BL/cj	0.07[c]/0.13	A	23	2.233	0.42	0.74	0.00		2.208/4.3	3
				B	42	2.128	0.50	0.68	0.00			
				C	83	2.183	0.72	1.34	1.21			
J1848+3219	TXS 1846+322	Q/cj	–0.16[a]/0.11	A	9	0.557	1.73	2.83	4.87		0.619/8.2	3
				B	21	0.600	1.41	2.31	3.66	+		
				C	30	0.623	1.15	1.48	2.93			
J1849+6705	S4 1849+67	Q/c	–0.20[c]/–0.06	A	22	1.240	0.83	2.07	1.71		1.280/7.4	8
				B	40	1.272	1.79	7.69	4.95	+		
				C	77	1.282	1.90	9.12	5.41	+		
J2147+0929	PKS 2144+092	Q/c	–0.09/0.03	A	11	0.782	2.25	7.83	6.49	+	0.983/16.3	5
				B	15	0.891	2.96	13.61	8.64	+		
J2157+3127	B2 2155+31	Q/c	–0.16/0.07	A	7	0.399	1.19	1.03	3.09		0.480/17.5	7
J2202+4216	BL Lac	BL/cj	0.17/0.31	A	10	2.950	1.16	15.04	2.99	+	3.506/21.8	3
				B	24	3.125	0.57	1.25	0.00			
J2203+1725	PKS 2201+171	Q/c	0.00/0.32	A	12	1.022	2.15	14.05	6.21	+	0.972/5.0	2
				B	18	0.953	2.27	9.99	6.48	+		
J2232+1143	CTA 102	Q/cj	–0.14/–0.42	A	7	4.605	0.53	1.48	0.00		4.794/2.4	2
				B	17	4.663	0.35	0.44	0.00			
J2253+1608	3C 454.3	Q/cj	–0.04/–0.11	A	12	10.417	0.54	2.11	0.00		10.390/6.1	7
J2327+0940	PKS 2325+093	Q/cj	–0.03[a]/–0.08	A	7	1.372	9.35	125.19	27.98	+	1.379/2.5	2
				B	18	1.419	1.02	2.35	2.23			

a – frequency range [300–10 500] MHz, b – frequency range [1000–10 000] MHz, c – frequency range [30–10 500] MHz, others have frequency ranges of [70–10 500] MHz, for $\alpha 1$ in column 4 of Table 3.

fit of the broad-band [70–10500] MHz data for the majority of sources, and the spectral index from two frequencies, 1.4 and 8.4 GHz, from the CRATES catalog (Combined Radio All-Sky Targeted Eight GHz Survey, Healey et al. 2007) except for three sources where the information is from NED; (5) symbols for different epochs (see Table 1); (6) effective number of flux measurements in IDV observations; (7) mean flux density in IDV observations; (8) the modulation index of IDV; (9) the reduced χ^2 of IDV; (10) the variability amplitude of IDV, with a zero given if $m \leq m_0$; (11) IDV identification, a "+" is given if the source shows IDV; (12) the mean flux density of the inter-month observations and the modulation index of inter-month variability; and (13) the effective number of measurements for inter-month variability.

As shown in Table 3, 26 sources (16 QSOs and 10 BL Lacs) show IDV at a confidence level larger than 99.9% at least once in the IDV observations, according to the χ^2 test. Thus the IDV occurrence is 26 out of 42 *Fermi* blazars, indicating that the IDV detection rate is $\sim$60%, which is higher than that in previous flat-spectrum AGN samples (e.g. Quirrenbach et al. 1992; Lovell et al. 2008). This high rate could be caused by a higher compactness of *Fermi* blazars relative to sources in other samples.

We find a pronounced inter-month variability in two BL Lac objects: J0112+2244 and J0238+1636, with a modulation index of 37.1% and 42.7%, respectively. Because the inter-month observation data are sparse and unevenly sampled, we will only use the 24 sources which have been observed at least 5 times for statistical results in the following.

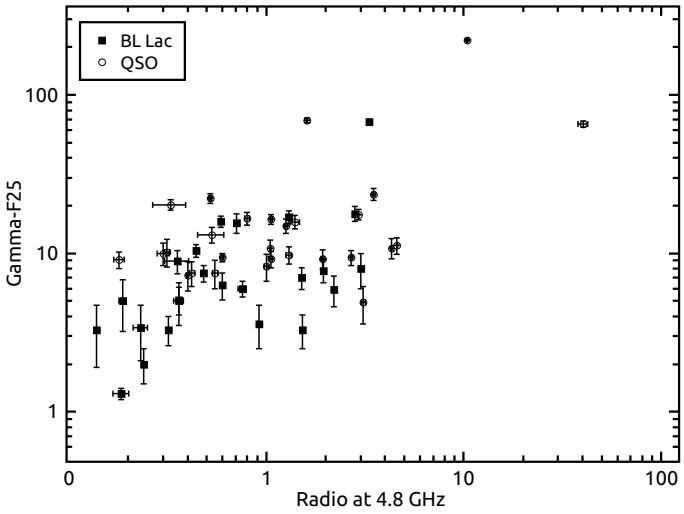

Fig. 2 Mean flux densities (averaged over all IDV sessions) and those from Table 2 at 4.8 GHz vs. the gamma-ray intensities ($\geq$100 MeV, in 10^{-8} ph cm^{-2} s^{-1}, from Abdo et al. 2009) of 52 *Fermi* blazars.

4.1 γ-ray and Radio Flux Density

The combined radio and γ-ray data can be used to study the relationship between radio and γ-ray emission. We find that there is a correlation between the 4.8 GHz radio flux density of 52 sources and their γ-ray intensity (Fig. 2) with a Spearman correlation coefficient of 0.48 (significance 2.8×10^{-4}) in total, 0.37 (significance 0.06) for QSOs and 0.61 (significance 0.001) for BL Lacs. For quasars the correlation does not seem to be significant, especially when removing the two strong quasars 3C 273 and 3C 454.3. However, there is still a correlation coefficient of 0.42 (significance 0.02) for 50 sources after dropping the two strong quasars. It is notable that our sample is incomplete and the radio-γ data are not simultaneous. The 15 GHz simultaneous radio-γ result obtained by the Caltech group (Readhead, private communication) shows a more significant correlation, where a new Monte-Carlo method was applied and an intrinsic correlation was found (also see Ackermann et al. 2011).

The correlation between radio and γ-ray emission in the blazars can shed light on the physical link between the emission processes in the two energy bands. It is suggested that the *Fermi*-LAT detected blazars have, on average, higher Doppler factors than non-*Fermi*-LAT detected blazars (Savolainen et al. 2010). It is possible that the γ-ray emission (via synchrotron self-Compton and/or inverse-Compton scattering by the relativistic electrons in the radio jet) from the *Fermi*-LAT detected blazars could also be Doppler-boosted.

4.2 Spectral Index and Flux Density Variability

It is possible that the 4.8 GHz flux density variability is related to the source spectral index. In order to obtain a more realistic estimate of the spectrum from broad-band radio data, we checked our 42 blazars in the SPECFIND V2.0 catalog of broadband [30–10 500] MHz radio continuum spectra (Vollmer et al. 2010), and obtained their indices, with the $\alpha1$ shown in Table 3. The frequency ranges of the spectra are [70–10 500] MHz for 27 sources, [300–10 500] MHz for 9 sources, [30–

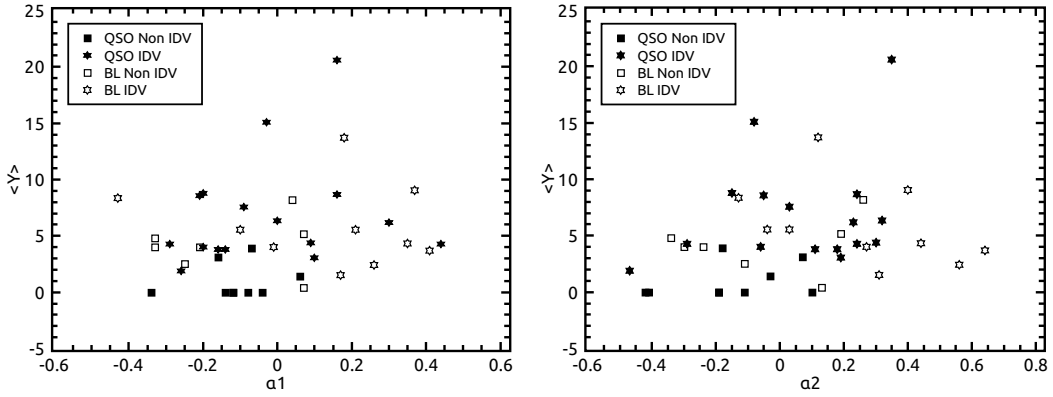

Fig. 3 IDV amplitude $\langle Y \rangle$ (averaged over all IDV sessions, except when $Y = 0$) versus spectral index ($\alpha 1$ from SPECFIND V2.0 and $\alpha 2$ from CRATES).

10 500] MHz for 5 sources, and [1000–10 000] MHz for 1 source. Although the spectral indices are from relatively low-frequency ranges, the 42 blazars still show flat spectral indices $\alpha 1 > -0.5$ from the SPECFIND V2.0 catalog. We also list the spectral index $\alpha 2$ calculated with 1.4 GHz and 8.4 GHz flux densities from the CRATES catalog in Table 3.

We plot the variability strength versus the spectral index for 42 blazars in Figure 3. No obvious correlation was found between the spectral index α (from either the SPECFIND V2.0 catalog or the CRATES catalog) and the variability amplitude $\langle Y \rangle$ of the IDV. The same results were obtained for inter-month variability (plot not shown here). However, it appears that the non-IDV blazars have spectral indices of $\alpha 1 < 0.1$ for the SPECFIND V2.0 and $\alpha 2 < 0.2$ (except one source with 0.26) for the CRATES 1.4/8.4 GHz spectral indices in Figure 3, suggesting that, in general, the non-IDV blazars have relatively "steeper" spectral indices than the IDV blazars.

4.3 IDV and Inter-month Variability

We tried to check whether there is a relationship between intra-day and inter-month variability, and used only the inter-month data observed over at least five months. No significant correlation was found for the sub-sample of 24 sources, however, better results could be expected for more sophisticated observations from a larger sample of sources in the future.

4.4 Variability Strength of QSOs and BL Lacs

We studied the different variability strength Y of IDV between QSOs and BL Lacs. Due to our incomplete sample, we calculated a median rather than a mean of the variability index. The result shows that the median is 3.96±4.92 for QSOs, and the median is 4.16±3.35 for BL Lacs. So there is no significant difference between QSO and BL Lac variability strength of IDV.

All 42 sources were observed by VLBI techniques, e.g. in the MOJAVE project (Monitoring Of Jets in Active galactic nuclei with VLBA Experiments, see Lister et al. 2009), and in the VCS project (VLBA Calibrator Survey, *http://astrogeo.org/vcs/*). We roughly checked the VLBI structures of the 42 blazars, and found that 14 out of the 16 type "c" blazars in Table 3 are IDV sources, suggesting that IDV occurs more often in the VLBI-core dominant blazars. There is no correlation between IDV variability and source redshift.

5 SUMMARY AND OUTLOOK

With the Urumqi telescope at 4.8 GHz, we measured the flux densities of 52 blazars and carried out IDV observations and inter-month flux monitoring for 42 blazars, from the first three months of the *Fermi*-detected AGN list. We summarize the results as follows:

(1) 26 IDV sources are detected at a high confidence level, and the IDV detection rate of $\sim 60\%$ in the *Fermi* blazar sample is higher than that in previous flat-spectrum AGN samples. The IDV appears more often in the VLBI-core dominant blazars.
– There is a correlation between the 4.8 GHz radio flux density and the γ-ray intensity for the 42 blazars as a whole, in which the correlation confidence is higher for BL Lacs than for quasars.
(2) Pronounced inter-month variability was found in two BL Lac objects: J0112+2244 and J0238+1636.
– No obvious correlation was found between the spectral indices and modulation indices of either intra-day or inter-month variability of the blazars. However, in general, the non-IDV blazars tended to have relatively "steeper" spectral indices than the IDV blazars.
– No significant correlation between the intra-day and inter-month variability was found in the data.
– No significant difference was found between the QSO and BL Lac variability strength of IDV in the current sample.

We are aware of the fact that this sample is small. Following the pilot studies presented in this paper, we launched a program to search for rapid variability in a large sample of radio sources with the Urumqi telescope in 2010, which uses the CRATES catalog as the parent sample to further investigate our findings. With this new project we plan to study in detail the statistics of IDV, a possible correlation between the occurrence of IDV and the presence of strong γ-ray emission, and the properties of γ-ray and non-γ-ray AGNs.

Acknowledgements We thank the referee for helpful comments and suggestions. This work is supported by the National Natural Science Foundation of China (Grant No. 11073036) and the National Basic Research Program of China (973 Program; 2009CB824800). This research has made use of data from the MOJAVE database that is maintained by the MOJAVE team (Lister et al. 2009).

References

Abdo, A. A., Ackermann, M., Ajello, M., et al. 2009, ApJ, 700, 597
Abdo, A. A., Ackermann, M., Ajello, M., et al. 2010, ApJ, 715, 429
Ackermann, M., Ajello, M., Allafort, A., et al. 2011, ApJ, 741, 30
Baars, J. W. M., Genzel, R., Pauliny-Toth, I. I. K., & Witzel, A. 1977, A&A, 61, 99
Benford, G. 1992, ApJ, 391, L59
Bevington, P. R., & Robinson, D. K. 1992, Data Reduction and Error Analysis for the Physical Sciences (New York: McGraw-Hill)
Bignall, H. E., Jauncey, D. L., Lovell, J. E. J., et al. 2003, ApJ, 585, 653
Dennett-Thorpe, J., & de Bruyn, A. G. 2000, ApJ, 529, L65
Gabányi, K. É., Marchili, N., Krichbaum, T. P., et al. 2009, A&A, 508, 161
Hartman, R. C., Bertsch, D. L., Bloom, S. D., et al. 1999, ApJS, 123, 79
Healey, S. E., Romani, R. W., Taylor, G. B., et al. 2007, ApJS, 171, 61
Heeschen, D. S., Krichbaum, T., Schalinski, C. J., & Witzel, A. 1987, AJ, 94, 1493
Kedziora-Chudczer, L., Jauncey, D. L., Wieringa, M. H., et al. 1997, ApJ, 490, L9
Kellermann, K. I., & Pauliny-Toth, I. I. K. 1969, ApJ, 155, L71
Kraus, A., Krichbaum, T. P., Wegner, R., et al. 2003, A&A, 401, 161

Lesch, H., & Pohl, M. 1992, A&A, 254, 29
Lister, M. L., Aller, H. D., Aller, M. F., et al. 2009, AJ, 137, 3718
Lovell, J. E. J., Rickett, B. J., Macquart, J.-P., et al. 2008, ApJ, 689, 108
Maraschi, L., Ghisellini, G., & Celotti, A. 1992, ApJ, 397, L5
Ott, M., Witzel, A., Quirrenbach, A., et al. 1994, A&A, 284, 331
Qian, S.-J., Li, X.-C., Wegner, R., Witzel, A., & Krichbaum, T. P. 1996, Chin. Astron. Astrophys., 20, 15
Quirrenbach, A., Witzel, A., Kirchbaum, T. P., et al. 1992, A&A, 258, 279
Readhead, A. C. S. 1994, ApJ, 426, 51
Rees, M. J. 1966, Nature, 211, 468
Savolainen, T., Homan, D. C., Hovatta, T., et al. 2010, A&A, 512, A24
Sun, X. H., Han, J. L., Reich, W., et al. 2007, A&A, 463, 993
Urry, C. M., & Padovani, P. 1995, PASP, 107, 803
Vollmer, B., Gassmann, B., Derrière, S., et al. 2010, A&A, 511, A53